Influence of Luminance L* in the L*a*b* Color Space during Color Segmentation in Highly Saturated Color Images

Rodolfo Alvarado-Cervantes[1], Edgardo M. Felipe-Riveron[2*], Vladislav Khartchenko[1] and Oleksiy Pogrebnyak[2]

[1] Centro de Investigaciones Teóricas, Facultad de Estudios Superiores Cuautitlán, Universidad Nacional Autónoma de México, Cuautitlán Izcalli, Mexico

[2] Instituto Politécnico Nacional, Centro de Investigación en Computación, Mexico

rodolfo.alvarado.cervantes@gmail.com; edgardo@cic.ipn.mx; vlad@unam.mx; olek@cic.ipn.mx

Abstract. In this paper a study of the influence of luminance L* at the CIE L* a* b* color space during color segmentation in highly saturated color images is presented. A comparative study is made between the behavior of segmentation in color images using (1) the Euclidean metric of the RGB channels (2) the Euclidean metric of a* and b* in CIE L*a*b* color space and (3) an adaptive color similarity function defined as a product of Gaussian functions in a modified HSI color space. For the evaluation, synthetic images were particularly designed to accurately assess the performance of the color segmentation. The testing system can be used either to explore the behavior of a similarity function (or metric) in different color spaces or to explore different metrics (or similarity functions) in the same color space. From the results it was obtained that the color parameters a* and b* are not independent of the luminance parameter L* as one might initially assume. In the majority of cases the CIE L*a*b color space was more influenced by the faded shadow than the RGB color space. The segmentation using the Euclidean metric in L*a*b* color space suffered errors in all cases. It manifested in different degrees and at different levels of faded shadow (less than 10% to 80%).

Keywords: Color image segmentation; CIE L*a*b* color space; color metrics; color segmentation evaluation; synthetic color image generation

---

* Corresponding author.

Rodolfo Alvarado-Cervantes, Edgardo M. Felipe-Riveron, Vladislav Khartchenko, et al.

1 Introduction

Image segmentation consists of partitioning an entire image into different regions, which are similar in some predefined manner. It is an important and difficult task in image analysis and processing. All subsequent steps, such as object recognition depend on the quality of segmentation [1].

For some time the development of segmentation algorithms attracted remarkable consideration compared with the relatively fewer efforts on their evaluation and characterization [2, 3, 4, 5]. Since none of the proposed automatic segmentation algorithms published is generally applicable to all types of images and different algorithms are not equally suitable for particular applications, the performance evaluation of segmentation algorithms and its characterization are very important subjects in the study of segmentation [3, 5].

Perceptual uniform color spaces such as CIE L*a*b*, with the Euclidean metric to quantify color distances are commonly used in color image segmentation of natural scenes using histogram based or clustering techniques among others [1].

To evaluate the segmentation performance of the Euclidean metric in the L*a*b color space, we designed a system that generated synthetic color images, with its associated ground truth (GT), and evaluated the results with Receiver operating characteristics (ROC) curves [7]. A short study of evaluation methods is presented in section 2. We present the evaluation system in section 3, where the synthetic images, designed to evaluate the efficiency of achieved color information from given segmentation algorithms are explained in detail. A comparative study between the behavior of segmentation in color images using (1) the Euclidean metric of the RGB channels (2) the Euclidean metric of a* and b* in the L*a*b* color space and (3) an adaptive color similarity function (defined as a product of Gaussian functions in a modified HSI color space [6]) is presented in section 4. Conclusions are given in section 5.

2 Previous Works

In recent years considerable effort has been devoted to the problem of color segmentation in digital images given its importance and potential. Until few years ago, the majority of published approaches for the segmentation of color were based on monochromatic techniques applied to each color component of the image in different color spaces (RGB or other) and in different ways to produce a color composite. These approaches have an inherent problem of significant loss of color information during the process [6].

The first comprehensive survey on evaluation methods of image segmentation is presented in Zhang (1996). It brings a coherent classification of existing methods at that time. Progress made in the subject during the five years after the first survey is presented in Zhang (2001). Another actualization is presented five years later[15] embracing together the principal methods of segmentation evaluation available up until 2007.

Zhang and others (2006) present a comprehensive survey on unsupervised methods of segmentation evaluation. The authors propose a hierarchy of published methods at that time by summarizing the main branches and locating the group of unsupervised methods on it. They mention their advantages, such as no requirement for GT to obtain quantitative results. They also propose the main lines of future research for this kind of methods.

Zhang and Gerbrands (1992) present a way to design synthetic images and a corresponding GT for evaluating segmentation algorithms. They introduce a general framework and general design considerations. They also present a system for generating synthetic images in shades of gray taking into account their design considerations. The behavior of a segmentation method in gray images using thresholding is studied and some remarks are obtained.

3 Design of Synthetic Images for Benchmark Testing

In [4] the authors present three important design considerations for creating synthetic images: 1. Synthetic images should be appropriate for a quantitative study and should allow objective evaluations of their properties; 2. The synthetic images should reflect the main features of real images, i.e. corruption factors, such as noise and blurring, variation of parameters such as size, shape, etc.; 3. The system should allow the generation of images with progressive variations of each parameter. In this way the study of the influence of each individual parameter is possible.

Comparative tests between: (1) the Euclidean metric using only a* and b* parameters in the L*a*b* color space [8], (2) the Euclidean metric of the RGB channels, and (3) the adaptive color similarity function presented in [6] were performed. The manner in which the tests were implemented is as follows:

In the case of the L*a*b* color space, the RGB image was previously transformed to L*a*b* color space discarding in all cases the luminance L* in order to calculate the Euclidean distance on the planes a*b* (color information) independently of the illumination. Then the centroid (average of the values a* and b*) representing the colors of the figure and the background in the color space L*a*b* was calculated. Details are shown in [8].

In the second case the Euclidean distance of the R, G and B color channels is calculated. The centroids are obtained taking the average of the values R, G, and B.

For the case (3) of the adaptive similarity function [6] the following steps were performed:

1. Samples of both background and figure were taken, from which centroid and standard color dispersion was calculated. Details can be consulted in [6] 2. The 24-bit RGB image (true color) was transformed to a modified HSI color space. 3. For each pixel, the similarity function to the centroids of figure and background was calculated creating two color similarity images (CSI) [6]. 4. Each pixel of the RGB image was classified by calculating the maximum value for each pixel position between the CSI images of the figure and that of the background.

The base shape of the synthetic test image was created with the following features:

1. Concave and convex sections in order to make it more representative of real images, such as natural flowers. 2. Extreme omnidirectional curvature in the entire image to hinder obtaining the edges applying mask edge detectors. 3. The object was centered in the image.

The resulting flower-shaped object in the image is considered as the object of interest and as the ground truth GT in all subsequent tests (Figure 1 left).
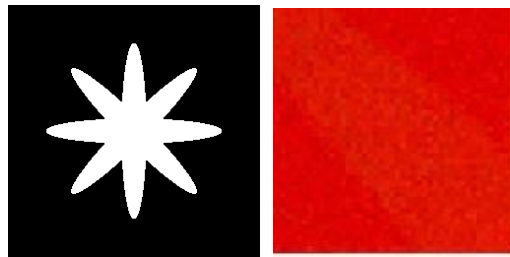

Fig. 1. Flower-shaped ground truth (left) and an image zoomed showing the introduced Gaussian noise (right)

In addition to this object of interest, several features were imposed in order to hinder its color-based segmentation:

1. Low contrast. The contrast between the object and the background in all images was very low for an observer, including some in which at a first glance the user cannot see the difference (e.g. Flower 5 in Figure 2). The difference between the color characteristics of the object of interest and the background we call "Delta" and it occurs at different directions of the HSI space. The tests were performed in color quadrants 0, 60, 120, 180, 240 and 300 degrees. 2. Blurred edges with an average filter. A sliding mean filter of size 3 x 3 pixels was applied to the whole image in order to blur the corners and to make object detection more difficult; this was done before the introduction of Gaussian noise. 3. Introduction of Gaussian noise with SNR value = 1 (Figure 1 right). The noise was applied to each of the RGB channels individually, and later we assembled the channels to create the RGB color image with noise. Figure 1 right shows an example.

The basic colors selected for both object and background were based on maintaining constant intensity to 0.9 and saturation to 0.9 and only varying the hue. Hue was selected as the parameter because its change integrates the three RGB color channels together, making it more difficult to be processed by extending grayscale techniques to each color channel, thus forcing the segmentation algorithms in evaluation to use the color information holistically.

Samples of pixels corresponding to the figure were obtained by two squares of 2 x 2 pixels starting at the pixel (84, 84) and (150, 150). Samples for background pixels were obtained by two squares of 2 x 2 pixels starting at pixel (15, 15) and (150, 180).

The images were generated in the sectors 0, 60, 120, 180, 240 and 300 degrees corresponding to the images flower_0, flower_1 … flower_5 (Figure 2). To these test images we later applied to each one a faded shadow in increments of 10% in each step.

Fig. 2. Testing with High Saturation with Delta in HUE

A shadow fading was applied to all noisy blurred images with the light center in the fixed coordinates (150,150) in images of 256 x 256 pixels. It was applied gradually with 10% increments in each step. Figure 3 shows this for Flower 0.


Fig. 3. Example in color quadrants with a faded shadow applied at 0 degrees

4 Results and Discussion

In this section we show the results in terms of TP (true positives) and FP (false positives) plotted against the level of shadow fading, representing each 10% step of increment. The first position means no shadow and position 11 means 100% shadow fading. All the images had the same post-processing: elimination of areas smaller than 30 pixels and a morphological closing with a circular structuring element of radius equal to two pixels.

The results of the application with the solution given by [6] of the color image segmentation with a different level of shadow fading (shown in every bottom row of each color) compared with those obtained with the Euclidean metric of the a* and b* parameters in the L*a*b color space (shown in every top row of every color) and the results obtained with the Euclidean metric of the RGB color channels (shown in every middle row of every color) are included in Figure 4 for each color quadrant (0°, 60°, 120°, 180°, 240° and 300°) and at 10% increments of the shadow fading.

As it is shown in the graphs in Figure 5 (plotting TP and FP of each level of faded shadow) and in coincidence with the visual analysis of the corresponding flower (see Figure 4), segmentation failures in the L*a*b* space start at different levels of faded shadow, whereas the color similarity function [6] is practically immune to the faded shadow (see Figure 6).
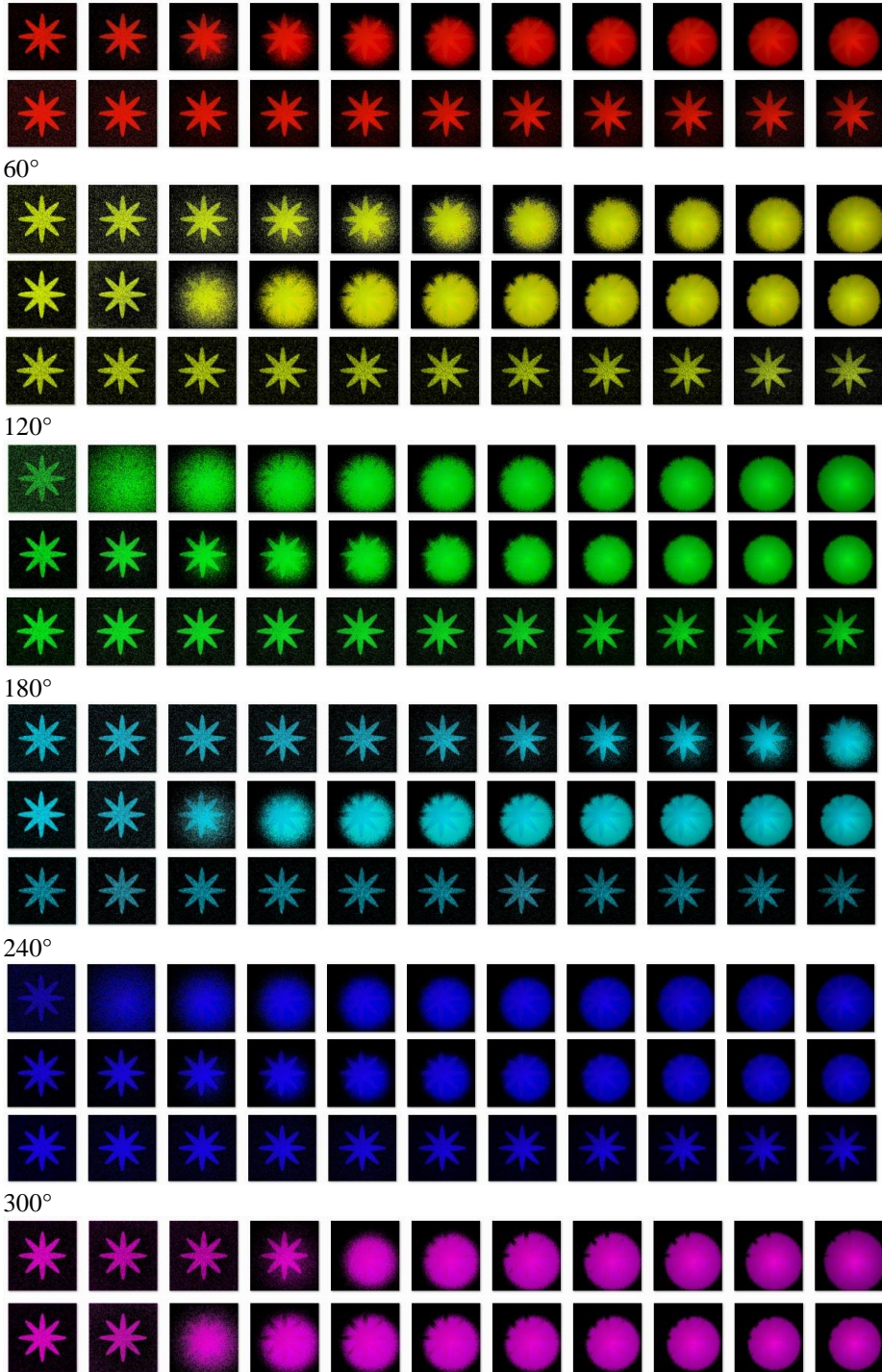
| 0% | 10% | 20% | 30% | 40% | 50% | 60% | 70% | 80% | 90% | 100% |
0°

60°

120°

180°

240°

300°
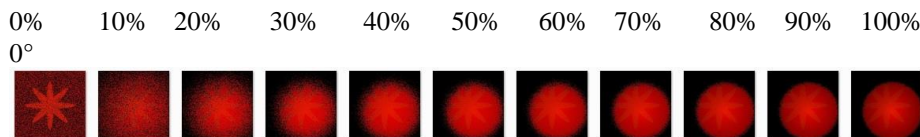
Fig. 4. Results of the color segmentation achieved between the Euclidean metric of the a* and b* parameters in the L*a*b* color space (top rows of each color), the Euclidean metric of the RGB color channels (middle rows of each color) and the adaptive color similarity function [6] (bottom rows of each color), for each color quadrant (0°, 60°, 120°, 180°, 240° and 300°) and at 10% increments of shadow fading in each step.

Three types of trends can be noticed in sectors with 120 degrees of difference: 1. Rise of the curve abruptly (Flowers 0, 2 and 4 which corresponds to the R G B color channels) with high sensibility to the faded shadow (higher than RGB); 2. Slow Rise (Flowers 1 and 5) lower than RGB, and 3 Insensitive increase (Flower 3) at near 90%. Table 1 summarizes the observations concerning the behavior of the plot curves comparing the Euclidean metric in L*a*b* color space, Euclidean metric in RGB, and the adaptive color similarity function [6].

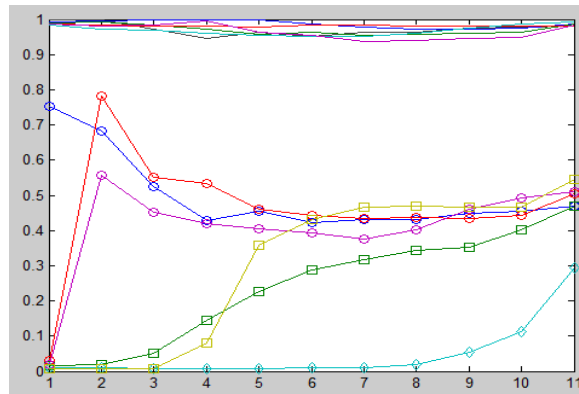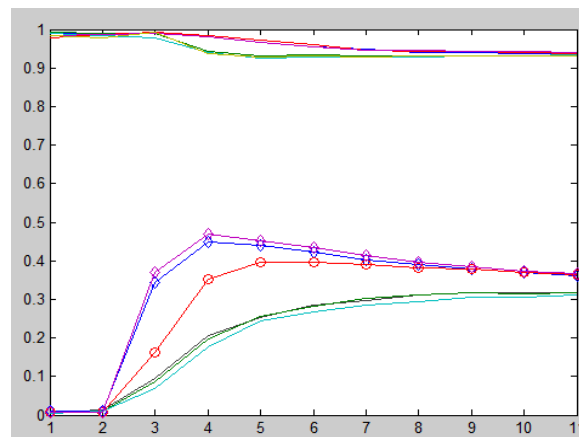**Fig. 5.** Plot of TP and FP using Euclidean metric of a* and b* parameters in L*a*b* color space

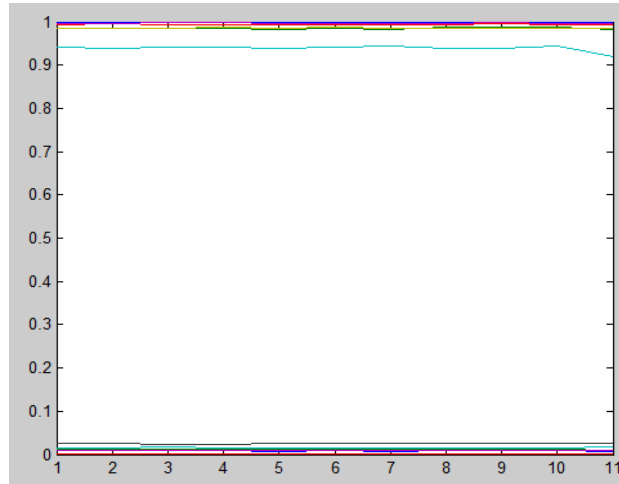**Fig. 6.** Plot of TP and FP using Euclidean metric of RGB

Fig. 7. Plot of TP and FP using the adaptive color similarity function [6]

Table 1. Observations concerning the behavior of the plot curves comparing L*a*b*, RGB, and an adaptive color similarity function

Flower	Line Color	Euclidean metric in L*a*b* rejecting L*	Euclidean metric in RGB	Color similarity function [6]
0	Blue	0% (position 1) Worst case	20% (position 3) Sharply increases	Immune
1	Green	30% (position 4) Increases slowly and progressively	30% (position 4) Increases slowly and progressively	Immune
2	Red	10% (position 2) Sharply increases	30% (position 4) Sharply increases	Immune
3	Cyan	80% (position 9) Increases at 45°	30% (position 4) Increases slowly and progressively	Immune
4	Purple	10% (position 2) Sharply increases	20% (position 3) Sharply increases	Immune
5	Yellow	30% (position 4) Sharply increases	30% (position 4) Increases slowly and progressively	Immune

To obtain representative ROC curves illustrating the behavior of the Euclidean metric in L*a*b* rejecting L*, the Euclidean metric of RGB and the adaptive color similarity function [6] in all color sectors under study, we calculated the average TP and FP for all color flowers, obtaining the results shown in Figures 8, 9 and 10.
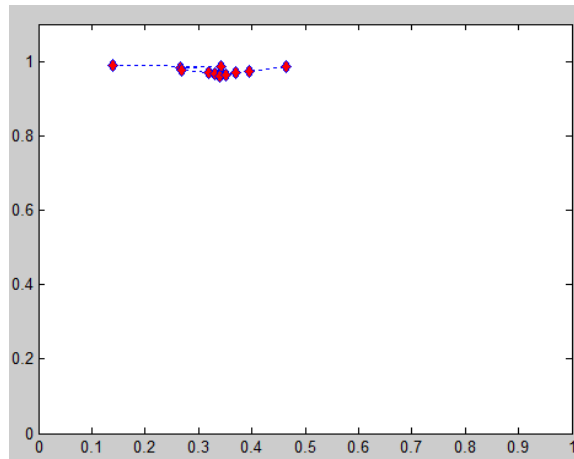
Fig. 8. ROC curve of Euclidean metric of a* and b* parameters in L*a*b* color space.
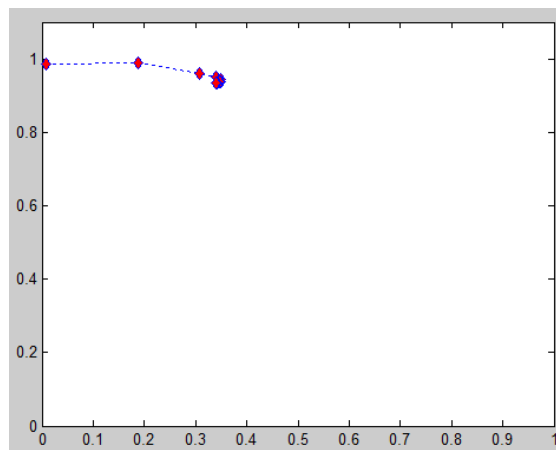

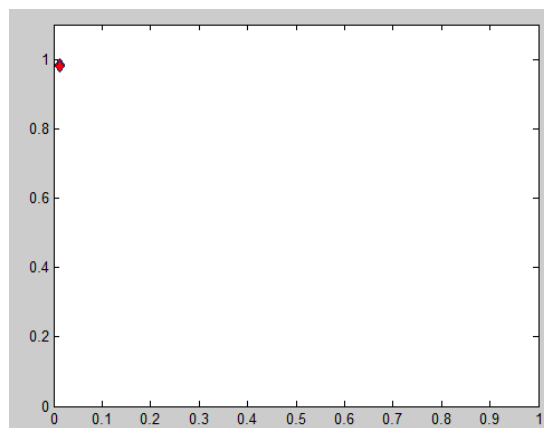**Fig. 9.** ROC curve of the Euclidean metric of RGB Channels

Fig. 10. ROC curve of the adaptive color similarity function [6]

In the ROC curve corresponding to the average of TP and FP of all flowers, it can be seen that the CIE L*a*b* results were poor from the beginning (worse than the RGB results) and continually moves to the upper right area of the ROC curve that can be thought of as the 'liberal' side (coordinate 1, 1) as they make positive classifications, and, although there is weak evidence that almost all positives were classified properly, they have a high rate of false positives.

The RGB results keep stable only the initial two steps and quickly moves to a point in the upper right area of the ROC curve that can be thought of as the 'liberal' side (coordinate 1, 1) as they make positive classifications, and, although there is weak evidence that almost all positives were classified properly, they have a high rate of false positives.

From the shown corresponding ROC curve it follows that the adaptive color similarity function is maintained in the high efficiency area (coordinate 0, 1) while the color segmentation in CIE L*a*b* space and the Euclidean metric of the RGB color channels progressively move away from the high efficiency area with a relatively small change in luminance L*.

5 Conclusions

Regarding the evaluation of the color segmentation method with really difficult conditions, we can notice that the segmentation algorithm using the CIE L*a*b* color space and discarding L* in calculating the Euclidean distance, suffered errors in all cases. It manifested in different degrees and at different levels of faded shadow (less than 10% to 80%). Three types of trends can be noticed in sectors with 120 degrees of difference: 1. Rise of the curve abruptly (Flowers 0, 2 and 4 which corresponds to the R G B color channels) with high sensibility to the faded shadow (higher than RGB); 2. Slow Rise (Flowers 1 and 5) lower than RGB, and 3 Insensitive increase (Flower 3) at near 90%.

The segmentation algorithm implementing the Euclidean metric of the RGB color channels maintained a similar and regular behavior with two types of trends: (1) sharp increase of errors manifested in this case in 20% to 30% of the fading shadow and (2) increases slowly and progressively in 3 cases.

The adaptive color similarity function performed well in all tests and remained close to the high efficiency zone of the ROC curves (coordinates 0, 1) without noticeable changes when the level of faded shadow increases as shown in the corresponding PLOT curves.

As it can be seen from the results of both direct segmentation, and from PLOT & ROC curves, the adaptive color similarity function in all cases exceeded: (1) The Euclidean distance in color space L*a*b* but discarding L* and the Euclidean metric of the R, G and B color channels and (2) the use of Euclidean distance of the RGB channels. The adaptive color similarity function performed well in all cases with rates higher than 95% of true positives (TP) and false positive (FP) rate less than 3% on average.

According to the experimental results we believe that keeping high values of TP increased only from the FP is due to the position of the center of the shadow fading in

(150, 150). If this position is moved away from the object of interest, we can reduce the quantity of TP.

In future work we wish to evaluate different color zones like with different saturations, gray images, and with delta saturation among others. Our testing system can be used either to explore the behavior of a similarity function (or metric) in different color spaces or to explore different metrics (or similarity functions) in the same color space. Instead of exchanging color spaces in the experiments, it would only be necessary to exchange the metric or the similarity function.

It can be noticed that the non-consideration of the luminance parameter L* in calculating Euclidean distance in the CIE L*a*b* color space (in each pixel of the object or of the background) did not made it immune to changes in lighting; so simple shadow can alter the quality of the results, concluding from them that the parameters a*b* from the CIE L*a*b* color space are not independent of the L* parameter as one might suppose.

References

1. Plataniotis, K.N., Venetsanopoulos, A.N.: Color Image Processing and Applications. First Edition, Springer, Berlin Heidelberg Germany; 354 p. (2000)
2. Zhang Y.J.: A Survey on Evaluation Methods for Image Segmentation. Pattern Recognition 29(8), 1335–1346 (1996)
3. Zhang, Y.J.: A review of recent evaluation methods for image segmentation. In :Proceedings of the 6th International Symposium on Signal Processing and Its Applications, pp. 148–151 (2001)
4. Zhang Y.J, Gerbrands J.J.: On the Design of Test Images for Segmentation Evaluation. In: Proceedings EUSIPCO 1, pp. 551–554 (1992)
5. Zhang Y.J.: A Summary of Recent Progresses for Segmentation Evaluation. In: Zhang Y.J. Advances in Image and Video Segmentation. IGI Global Research Collection, Idea Group Inc (IGI), pp. 423–439 (2006)
6. Alvarado-Cervantes R., Felipe-Riveron E.M., Sanchez-Fernandez L.P.: Color Image Segmentation by means of a Similarity Function. In: 15th Iberoamerican Conference on Pattern Recognition, CIARP 2010, Rodolfo Alvarado-Cervantes, Edgardo M. Felipe-Riveron y Luis P. Sánchez-Fernandez, I. Bloch, R.M. Cesar, Jr. (Eds.): Sao Paulo, Brazil, November 8-11, 2010, LNCS 6419, pp. 319–328, Springer, Heidelberg (2010)
7. Fawcett T.: An introduction to ROC analysis. Pattern recognition Letters 27: 861–874 (2006)
8. http://www.mathworks.com/help/images/examples/color-based-segmentation-using-the-l-a-b-color-space.html (Revised on April 27, 2015)